



Catalytic oxidation of aqueous sulfide in the presence of ferrites (MFe₂O₄, M = Fe, Cu, Co)



Igor T. Cunha^a, Ivo F. Teixeira^b, Adriana S. Albuquerque^c, José D. Ardisson^c, Waldemar A.A. Macedo^c, Henrique S. Oliveira^a, Juliana C. Tristão^d, Karim Sapag^e, Rochel M. Lago^{a,*}

^a Chemistry Department UFMG, Belo Horizonte, MG, Brazil

^b Department of Chemistry, University of Oxford, Oxford, UK

^c Applied Physics Lab, CDTN, Belo Horizonte, MG, Brazil

^d Chemistry Department UFV, Florestal, MG, Brazil

^e Physics Department Universidad Nacional de San Luis, Argentina

ARTICLE INFO

Article history:

Received 17 March 2015

Received in revised form 2 July 2015

Accepted 17 July 2015

Available online 19 August 2015

Keywords:

Ferrite

Sulfide oxidation

Polysulfide

ABSTRACT

In this work, the spinel structured iron oxides, MFe₂O₄ (M = Cu²⁺ and Co²⁺), magnetite (Fe₃O₄) and maghemite (γ-Fe₂O₃) were investigated as catalyst for the sulfide oxidation in aqueous medium. XRD, Mössbauer, BET, TPR, SEM/EDS and XPS analyses suggest the formation of the spinel phase with surface areas varying from 75 to 105 m² g⁻¹ and the metal ions Cu²⁺ and Co²⁺ located in the octahedral and tetrahedral sites. It was observed that the presence of Co and especially Cu strongly increased the catalytic activity for the oxidation of sulfide to polysulfides, i.e. S_x²⁻ (x = 1–4) and other S–O species. The strong effect of Cu²⁺ is discussed in terms of thermodynamically favorable processes comprising a strong surface interaction of S²⁻–Cu²⁺, an electron transfer from sulfide to produce Cu¹⁺ followed by an electron transfer from Cu¹⁺ to Fe³⁺_{bulk}.

© 2015 Elsevier B.V. All rights reserved.

1. Introduction

Sulfides are present in wastewaters from different industries, such as oil refineries, fossil fuel gasification plants, paper mills and anaerobic treatment plants. In aqueous medium, even in very low concentrations, sulfide will form the unpleasant and toxic hydrogen sulfide, causing corrosion problems in equipment and constructions [1,2]. Therefore, there is a considerable interest on the development of efficient and low cost systems for the removal of sulfide from gas and specially from aqueous phase [3].

The removal of sulfide has been investigated using different methods such as adsorption, biological processes and catalytic oxidations. Several works have been investigating the removal of H₂S using different adsorbents such as activated carbon [4,5], alumina [6], silica [7] and zeolite [8]. Microorganisms can be used to oxidize sulfide into sulfur-containing species, e.g. elemental sulfur, polysulfides, thiosulfate, thionates and sulfate in aqueous medium [9–11]. Furthermore, different biological processes to remove sulfide have been proposed, e.g. biofilters [12] and microorganisms supported

on activated carbon (AC) have been investigated for sulfide removal [13].

Oxidation of H₂S in the gas phase at high temperature with different catalysts, such as TiO₂, Cr₂O₃, V₂O₅, Fe₂O₃, have been reported [14]. However, no catalytic process was developed for aqueous sulfide. Recent studies have shown that modified carbon based materials, e.g. activated carbon, graphite and graphene, are active for sulfide oxidation in aqueous medium [15,16]. Based on these works and other enzyme promoted sulfide oxidation, it was suggested that two features are important for an active system, i.e. a surface redox group to exchange electrons with sulfide species and an electron conducting structure to promote the oxidation. In this work, it was investigated for the first time ferrites with special redox properties as catalysts for the sulfide oxidation in aqueous medium. Ferrites have a great potential for aqueous sulfide oxidation, because they have an excellent redox pair based on Fe²⁺/Fe³⁺, and a conducting solid structure able to disperse electrons. Moreover, ferrites can be isostructurally doped with different transition metals, e.g. Cu²⁺, Co²⁺, Mn²⁺, Ni²⁺, allowing a fine tuning of the catalytic/redox activity [17–20], electrical [21,22] and magnetic properties [19,23]. Moreover, ferrites show some potential advantages such as relatively low cost, improved chemical and thermal stability (compared to enzymes), excellent control of the structure

* Corresponding author.

E-mail addresses: jdr@cdtn.br (J.D. Ardisson), rochel@ufmg.br (R.M. Lago).

allowing fine tuning of the redox properties (compared to modified carbon based catalysts that are complex structures). Another interesting feature of ferrites is the magnetic property which can be used to remove the catalyst from the reaction medium by a simple magnetic process.

Hereon, different iron oxides with the same spinel structure, i.e. ferrites MFe_2O_4 ($M = Cu^{2+}$ and Co^{2+}), magnetite (Fe_3O_4) and maghemite ($\gamma-Fe_2O_3$) were investigated as catalyst for the catalytic activity in the aqueous sulfide oxidation.

2. Experimental

The ferrites samples were synthesized by co-precipitation process using Fe(III), Cu(II) and Co(II) nitrates (Synth) dissolved in deionized water in the required proportion to obtain the ferrites MFe_2O_4 ($M = Co$ or Cu). After 1 h with a magnetic stirring (approximately 60 rpm) at room temperature (25 °C), it was added NaOH (3.5 M) until pH 8, the precipitate was filtered, washed with deionized water and acetone and dried at 70 °C for 24 h. The obtained powder was treated at 400 °C during 2 h in air to obtain the crystalline ferrite phases, following the procedures described in a previous study [24]. Magnetite was prepared by co-precipitation of Fe(III) and Fe(II) nitrates (Synth) using the same conditions. Maghemite was prepared by the oxidation of Fe_3O_4 with air heating 10 °C/min at 400 °C for 1 h.

The catalysts were characterized by X-ray diffraction using a Geigerflex Rigaku diffractometer (Cu K α radiation). The transmission ^{57}Fe Mossbauer measures were obtained at 25 K on a constant acceleration transducer with a $^{57}Co/Rh$ source. The Normo least-square fits was employed to calculate the spectral hyperfine parameters. XPS analysis was conducted with a non-monochromatic Mg K α X-ray source ($h\nu = 1253.6$ eV), Al K α X-ray source ($h\nu = 1486.6$ eV) and a hemispherical concentric analyzer (CLAM2 – VG Microtech). The binding energies were corrected through C (1s) reference peak at 284.6 eV. The temperature programmed reduction (TPR) analysis was performed in a CHEM BET 3000 TPR Quantachrome using H_2 (5% in N_2) with heating rate of 10 °C min^{-1} . SEM/EDS analysis was done using a Jeol JSM 840A and a Quanta 200 ESEM FEG from FEI. The surface area was determined by nitrogen adsorption using the BET method with a 22 cycles N_2 adsorption/desorption in an Autosorb 1 Quantachrome instrument. X-band electron paramagnetic resonance (EPR) spectra from samples at room temperature were recorded on a Bruker Elexsys E500 spectrometer equipped with a Bruker ER4122SHQE resonator. Magnetization measurements were performed using a vibrating sample magnetometer (LakeShore 7404), with noise base of 1×10^{-6} emu, and a time constant of 300 ms at room temperature and a maximum magnetic field of 2 Tesla.

The sulfide oxidation studies were performed using 10, 15 and 20 mg of sample in 3 mL of $Na_2S \cdot 9H_2O$ (8 g L^{-1}) solution in water, i.e. concentrations in the range 3.3–6.6 mg $_{ferrite}/mL_{Na_2S}$. During the experiments, the formation of polysulfides was monitored by measuring the absorbance of the aqueous solution at a wavelength of 270 nm using a Shimadzu UV-2550 Spectrometer.

3. Results and discussion

The catalysts prepared in this work were Fe_3O_4 (magnetite), Fe_2O_3 (maghemite) and the ferrites $CuFe_2O_4$ and $CoFe_2O_4$. Magnetite has the redox pair (Fe^{2+}/Fe^{3+}), whereas the ferrites offer different possibilities for redox processes at the surface, e.g. ($Cu^{2+}/Cu^+/Fe^{2+}/Fe^{3+}$) and ($Co^{2+}/Co^{3+}/Fe^{2+}/Fe^{3+}$), as demonstrated by XPS (Fig. S1) [25]. The maghemite shows the same magnetite structure (spinel), but no Fe^{2+} in the structure. Fig. 1 shows X-ray diffractograms for the synthesized materials.

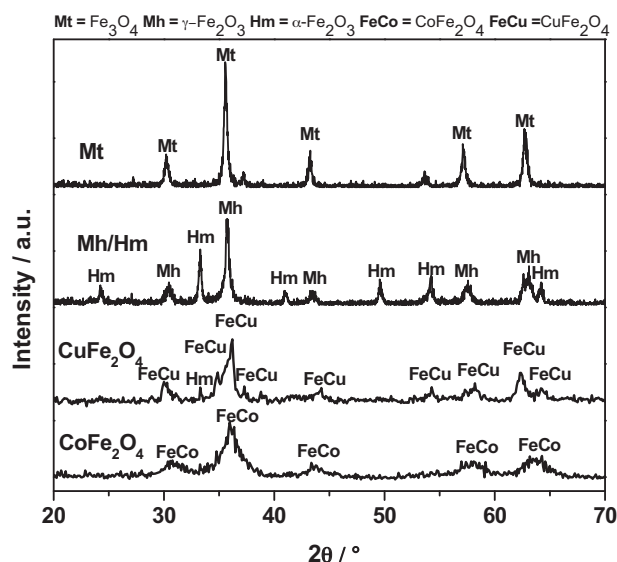


Fig. 1. XRD for the samples Mt (magnetite), Mh (maghemite), $CuFe_2O_4$ and $CoFe_2O_4$ (ferrite).

The maghemite sample was prepared by the oxidation of Fe_3O_4 in order to produce a material with similar surface area and porosity. During this process the Fe_3O_4 phase is oxidized to $\gamma-Fe_2O_3$ (maghemite) which is in part converted to the hexagonal phase hematite $\alpha-Fe_2O_3$. The XRD data suggests that maghemite sample is composed mainly of $\gamma-Fe_2O_3$ (maghemite) (JCPDF 39-1346) and some hexagonal hematite phase $\alpha-Fe_2O_3$ (JCPDF 13-534). This structural change maghemite-hematite at 400 °C has been observed before [26].

The samples Mt, $CuFe_2O_4$ and $CoFe_2O_4$ showed only the diffraction peaks of the spinel phases (JCPDF 19-629, 6-545 and 1-1121). Samples Mt and Mh/Hm showed more intense and better defined peaks, indicating a higher crystallinity with crystallite average size between 20 and 25 nm as estimated by the Scherrer equation. The XRD of the ferrites showed poorly defined peaks indicating that both materials have low crystallinity with crystallite sizes between 4 and 10 nm.

Mössbauer spectra at 25 K are shown in Fig. 2 (see Supplementary Material for the hyperfine parameters).

The sample Mt showed typical hyperfine parameters of magnetite, whereas maghemite presented two phases $\alpha-Fe_2O_3$ and $\gamma-Fe_2O_3$, as also shown by XRD. This result suggests that during thermal treatment maghemite was partially converted to hematite. Mössbauer spectra of the ferrites $CuFe_2O_4$ and $CoFe_2O_4$ indicated the presence of Fe^{3+} distributed in tetrahedral (A) and octahedral sites (B). These results show that the ions Co^{2+} and Cu^{2+} are located in both, octahedral and tetrahedral sites according to the simplified formula: $(Fe^{3+}_{1-x}M^{2+}_x)_{tetrahedral}(Fe^{3+}_{1+x}M^{2+}_{1-x})_{octahedral}O_4$ being x the inversion parameter, varying from 0 to 1. Mössbauer spectra obtained at room temperature suggested a strong superparamagnetism due to the nanostructured ferrites. In addition, the catalysts $CuFe_2O_4$ and $CoFe_2O_4$ were submitted to magnetization measurements by VSM (see Supplementary Material). Both materials showed similar magnetization curves suggesting the presence of supermagnetic materials (see Supplementary Material). These ferrites have been previously investigated in detail by Mössbauer spectroscopy [24,25].

The synthesized samples showed similar surface areas, i.e. 75, 72, 100, 104 $m^2 g^{-1}$ for Mt, Mh/Hm, $CoFe_2O_4$ and $CuFe_2O_4$, respectively, obtained by nitrogen adsorption using the BET method.

The obtained Fe oxides were tested for oxidation of aqueous sulfide. The non-colored sulfide solution became immediately light

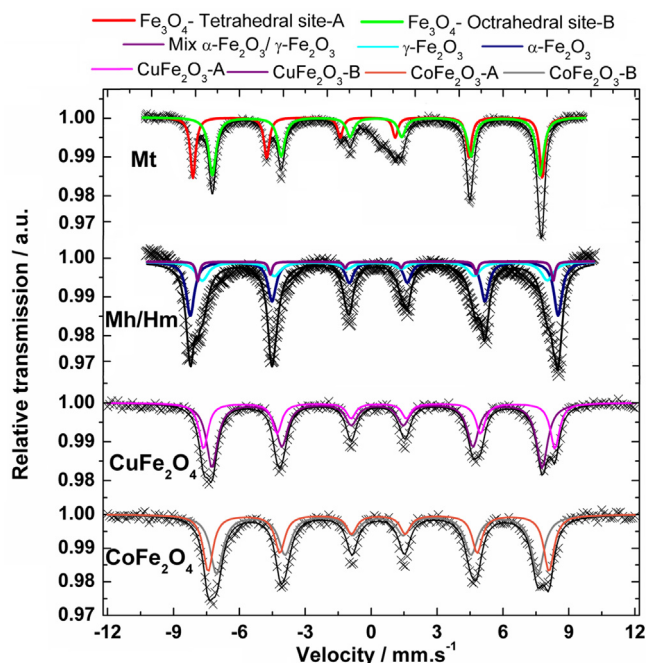


Fig. 2. Mössbauer spectra (at 25 K) for Mt, Mh/Hm, CuFe_2O_4 and CoFe_2O_4 . In red the tetrahedral sites (A) and in green the octahedral sites (B). (For interpretation of the references to color in this figure legend, the reader is referred to the web version of the article.)

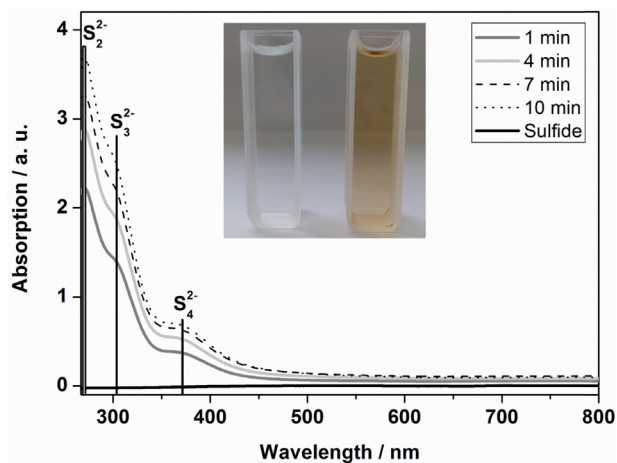


Fig. 3. UV/Vis spectra evolution during the sulfide oxidation in the presence of CuFe_2O_4 (UV/Vis spectra for the other catalysts not shown).

yellow in the presence of the ferrites. The UV/Vis spectra (Fig. 3 and Supplementary Material) of the sulfide solution gradually showed characteristic bands for small polysulfides species, such as S_2^{2-} (270 nm) [27], S_3^{2-} (300 nm) [27], S_4^{2-} (370 nm) [27]. The catalyst concentration was adjusted to 3.3 mg/mL in order to obtain accurate UV/Vis measurements.

The sulfide oxidation apparently takes place by the formation of polysulfides such as S_2^{2-} and S_3^{2-} , which can be identify by absorption bands on UV/Vis spectrum in the region of 270 and 290 nm whereas the band at 370 nm is likely related to S_4^{2-} , as highlighted by a recent work using carbon based catalysts [27]. Subsequently to the formation of polysulfides, the oxidation continues to form a complex mixture of oxygenated sulfur species [15]. In order to investigate the formation of anion radicals, such as $\text{S}_n^{\cdot-}$, which have been observed previously [15,28] several EPR measurements

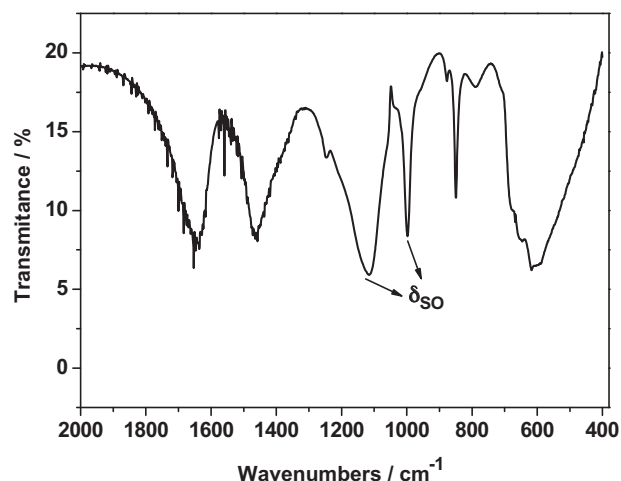


Fig. 4. Infrared spectrum of the solid product obtained after evaporation at 25 °C under vacuum of the solution resulting from oxidation of sulfide by CuFe_2O_4 .

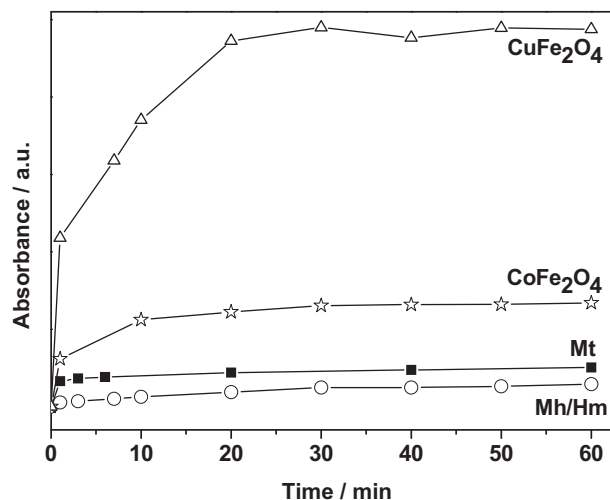


Fig. 5. Kinetic of polysulfides formation (band in 270 nm) during oxidation reaction of Na_2S with different Fe oxide catalysts.

during reaction were carried out. No EPR signal could be observed suggesting that radicals are not involved in the reaction.

The resulting solution of the reaction with the ferrite CuFe_2O_4 was evaporated under vacuum at room temperature (25 °C) and the product, a pale yellow solid, was characterized by infrared spectroscopy (Fig. 4).

The IR spectrum shows strong bands at 1006 cm^{-1} and 1105 cm^{-1} , both related to the axial symmetric deformation of $\text{S}=\text{O}$ [29,30].

The sulfide oxidation kinetics was accompanied by the UV band at 270 nm. The obtained results for Mt, Mh, CuFe_2O_4 and CoFe_2O_4 are shown in Fig. 5.

It can be observed that CuFe_2O_4 presented the highest activity for the oxidation reaction. The absorbance at 270 nm increased until approximately 30 min and remained stable thereafter. The sample CoFe_2O_3 showed lower polysulfide formation with significant activity in the first 10 min. Similarly, Mt and Mh/Hm showed much lower activity, suggesting that Co and specially Cu are playing an important role in the reaction.

The reuse of the CuFe_2O_4 catalyst was investigated in consecutive reactions, where after the first reaction the ferrite was simply removed magnetically from the reaction medium and reused

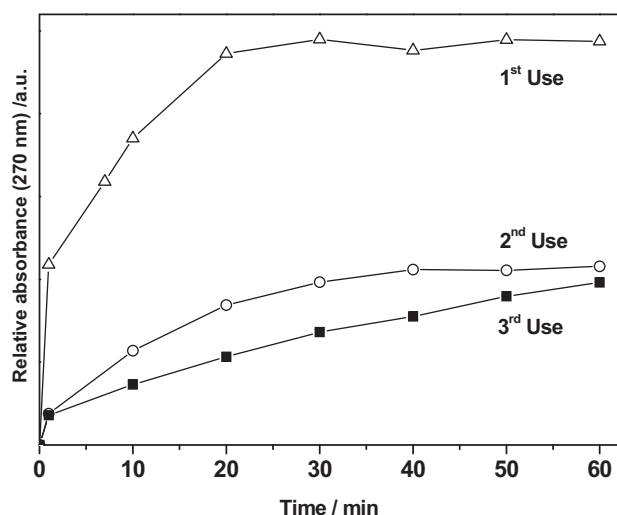


Fig. 6. Kinetic of formation for polysulfides (band in 270 nm) during oxidation reaction of Na_2S to reuse of CuFe_2O_4 ferrite.

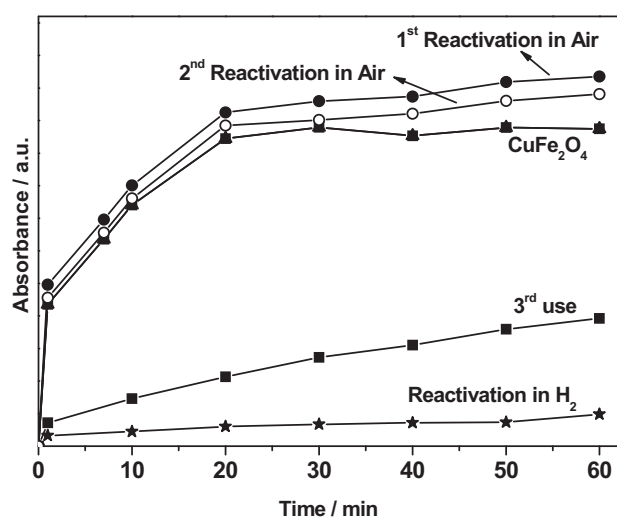


Fig. 7. Polysulfide formation (at 270 nm) during Na_2S reaction after 3 consecutive uses followed by two reactivation treatments, i.e. by H_2 and by oxidation in air.

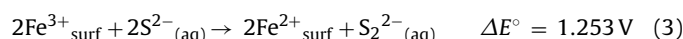
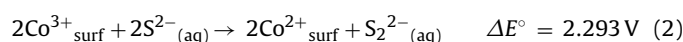
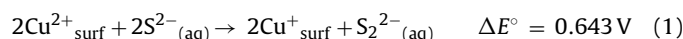
directly for another reaction with fresh Na_2S solution without any treatment. The obtained kinetics are shown in Fig. 6.

The 2nd and 3rd uses showed considerable decrease in the formation of polysulfide. EDS analyses of the CuFe_2O_4 catalyst after the 3rd use and extensive washing with water showed the presence of a strong sulfur signal suggesting a surface poisoning (Fig. S4).

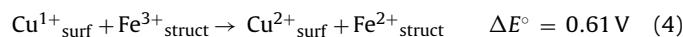
The regeneration of the reused CuFe_2O_4 catalyst was investigated using different methods. Treatment by water at pH 5 and 9 did not show any significant regeneration. It was also carried out a reactivation applying two different thermal treatments to the sample after the 3rd use. The first was under an atmosphere of H_2 at a heating rate of $10^\circ\text{C}/\text{min}$ to a final temperature of 400°C . The second method of reactivation was realized under an atmosphere of Air at a heating rate of $10^\circ\text{C}/\text{min}$ to a final temperature of 400°C . In addition, after the first reactivation under an air atmosphere and obtaining of the UV–Vis spectra, the catalyst was magnetically separated from the solution and a second reactivation under air atmosphere up to a final temperature of 400°C was realized. The profiles of reaction for the CuFe_2O_4 ferrite, the 3rd use and the reactivated ferrites are shown in Fig. 7.

As noted by the kinetic curves, reactivation in a reducing atmosphere of H_2 was insufficient to retake the initial activity of the ferrite likely due to the reduction of Fe and Cu active species and the incapability of the thermal treatment to eliminate the sulfur bonded in the surface of the ferrite (Fig. S4). On the other hand, the reactivation in air atmosphere generated a satisfactory regeneration of the catalyst, being able to eliminate the sulfur poisoning the surface of the ferrite. In addition, even the second reaction under air atmosphere was able to regenerate the activity of the catalyst. As a result, this reactivation process can be considered as a suitable mechanism to improve the reuse of the catalyst, increasing its active life-cycle.

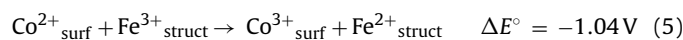
Although the reaction mechanism is not clear, some simple considerations can be made in order to explain the higher activities observed for the Co and especially Cu ferrites. An important reaction step is likely the electron transfer from S_2^{2-} to surface Fe^{3+} , Co^{3+} (observed on the surface by XPS [25]) or Cu^{2+} (Eqs. (1)–(3)).



Considering the redox potentials, the sulfide oxidation with copper should be the less favorable system ($\Delta E^\circ = 0.643 \text{ V}$) whereas cobalt should produce the most favorable reaction ($\Delta E^\circ = 2.293 \text{ V}$). However, these results suggest that the rate-determining step in this reaction is not the electron transfer from S_2^{2-} to the surface metal cation. Based on redox property of ferrite, the reduced $\text{Cu}^{+}_{\text{surf}}$ can easily transfer electrons to bulk Fe^{3+} species [31,32], which are present in material structure according to the simplified process shown in Eq. (4):



This process should be thermodynamically favorable, judging by the standard ΔE° value (0.61 V). On the other hand, the electron transfer from cobalt reduced species $\text{Co}^{2+}_{\text{surf}}$ (Eq. (2)) to bulk Fe^{3+} is not a favorable process, as shown in the simplified Eq. (5):



Therefore, a possible reason to explain the higher CuFe_2O_4 activity is that the electron transfer from the reduced surface metal, Cu^{1+} might influence the reaction rate. Although the destination of these electrons present in the ferrite structure is not clear, some possible reactions are the reduction of H_2O or O_2 which are well known to take place by Fe^{2+} present in the oxide structures [33–36] (Eqs. (6) and (7)):



It should also be considered the first interaction of the aqueous sulfide with the metal cations, Fe^{3+} , Cu^{2+} and Co^{3+} present on the ferrite surface. The first sulfide oxidation likely takes place by the replacement of a surface M–O bond to form a M–(S^{2-}) followed by an electron transfer (Fig. 7). A simple measurement of this S^{2-} interaction with surface metal cations was obtained considering the solubility products (K_{sp}) for the different sulfides CuS (10^{-38}), Cu_2S (10^{-47}), CoS (10^{-22}) and FeS (10^{-19}) [37]. It can be observed that both Cu^{+1} and Cu^{+2} have much stronger affinity for sulfide compared to Co and Fe. This affinity should likely contribute to the activity of the ferrite for the sulfide oxidation.

Although the mechanism of the oxidation has not been completely clarified, the aspects previously mentioned generate indication to elucidate a schematic representation of the steps involved in the oxidation process. They cover the interaction of the

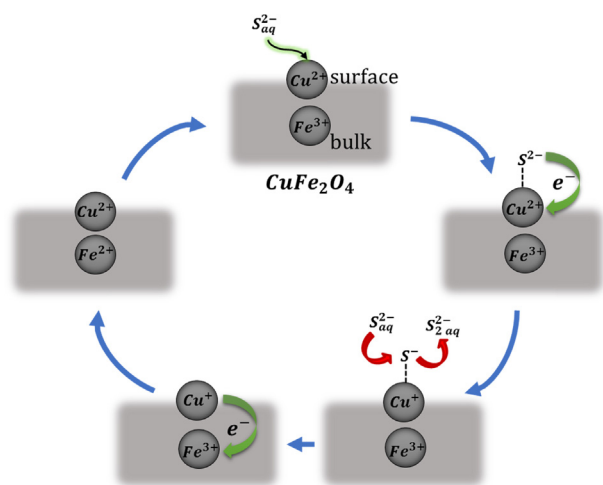


Fig. 8. Schematic representation of a mechanism proposal for the electron transfer through the ferrite CuFe_2O_4 conducting surface.

sulfide with the superficial cations; the redox process occurring in the internal structure of the ferrites; the dispersion of electrons to the solution; and the formation of polysulfide species. Therefore, Fig. 8 presents a simplified reaction mechanism for the proposed process of sulfide oxidation.

Details of the reaction mechanism is under investigation using XPS to study the changes in oxidation states of surface species including the metals and different types of sulfides and also ESI-MS (Electrospray ionization mass spectrometry) to identify the different polysulfide species in aqueous solution.

4. Conclusions

Sulfide, it is an important issue regarding water treatment and management. The ferrites previously synthesized and described in this paper, especially CuFe_2O_4 demonstrated a considerable activity in the promotion of sulfide oxidation. This ferrite comprises several aspects highlighted as necessary for the reaction: (i) the redox surface site able to oxidize the sulfide and (ii) the conducting properties necessary to disperse the electrons. These results bring new and relevant information for the development of new catalysts for the oxidation of aqueous sulfide.

Acknowledgements

The authors acknowledge the support of Petrobras, FAPEMIG, PRPq/UFMG, CNPq and CAPES. Thanks for the SEM/EDS provided by the UFMG Microscopy Center.

Appendix A. Supplementary data

Supplementary data associated with this article can be found, in the online version, at <http://dx.doi.org/10.1016/j.cattod.2015.07.023>

References

- [1] J.E. Burgess, S.A. Parsons, R.M. Stuetz, Developments in odour control and waste gas treatment biotechnology: a review, *Biotechnol. Adv.* 19 (2001) 35–63.
- [2] G. Tchobanoglous, F.L. Burton, H.D. Stensel, *Wastewater Engineering: Treatment and Reuse*, New York, 2003.
- [3] L. Zhang, P. De Schryver, B. De Gussem, W. De Muynck, N. Boon, W. Verstraete, Chemical and biological technologies for hydrogen sulfide emission control in sewer systems: a review, *Water Res.* 42 (2008) 1–12.

- [4] Y. Elsayed, M. Seredych, A. Dallas, T.J. Bandosz, Desulfurization of air at high and low H_2S concentrations, *Chem. Eng. J.* 155 (2009) 594–602.
- [5] K. Sakanishi, Z.H. Wu, A. Matsumura, I. Saito, T. Hanaoka, T. Minowa, M. Tada, T. Iwasaki, Simultaneous removal of H_2S and COS using activated carbons and their supported catalysts, *Catal. Today* 104 (2005) 94–100.
- [6] J.W. Bae, S.-H. Kang, G. Murali Dhar, K.-W. Jun, Effect of Al_2O_3 content on the adsorptive properties of $\text{Cu/ZnO/Al}_2\text{O}_3$ for removal of odorant sulfur compounds, *Int. J. Hydrogen Energy* 34 (2009) 8733–8740.
- [7] Y. Belmabkhout, G. De Weireld, A. Sayari, Amine-bearing mesoporous silica for CO_2 and H_2S removal from natural gas and biogas, *Langmuir* 25 (2009) 13275–13278.
- [8] A. Alonso-Vicario, J.R. Ochoa-Gómez, S. Gil-Río, O. Gómez-Jiménez-Aberasturi, C.A. Ramírez-López, J. Torrecilla-Soria, A. Domínguez, Purification and upgrading of biogas by pressure swing adsorption on synthetic and natural zeolites, *Microporous Mesoporous Mater.* 134 (2010) 100–107.
- [9] A. Vairavamurthy, B. Manowitz, W.Q. Zhou, Y.S. Jeon, Determination of hydrogen-sulfide oxidation-products by sulfur K-edge X-ray-absorption near-edge structure spectroscopy, in: C.N. Alpers, D.W. Blowes (Eds.), *Environmental Geochemistry of Sulfide Oxidation*, 1994, pp. 412–430.
- [10] M.R. Hoffmann, B.C. Lim, Kinetics and mechanism of the oxidation of sulfide by oxygen – catalysis by homogeneous metal–phthalocyanine complexes, *Environ. Sci. Technol.* 13 (1979) 1406–1414.
- [11] O. Weres, L. Tsao, R.M. Chhatre, Catalytic-oxidation of aqueous hydrogen-sulfide in the presence of sulfite, *Corrosion* 41 (1985) 307–316.
- [12] H.Q. Duan, R. Yan, L.C.C. Koe, X.L. Wang, Combined effect of adsorption and biodegradation of biological activated carbon on H_2S biotrickling filtration, *Chemosphere* 66 (2007) 1684–1691.
- [13] Y.L. Ng, R. Yan, X.G. Chen, A.L. Geng, W.D. Gould, D.T. Liang, L.C.C. Koe, Use of activated carbon as a support medium for H_2S biofiltration and effect of bacterial immobilization on available pore surface, *Appl. Microbiol. Biotechnol.* 66 (2004) 259–265.
- [14] X. Zhang, G. Dou, Z. Wang, L. Li, Y. Wang, H. Wang, Z. Hao, Selective catalytic oxidation of H_2S over iron oxide supported on alumina-intercalated Laponite clay catalysts, *J. Hazard. Mater.* 260 (2013) 104–111.
- [15] B.R.S. Lemos, I.F. Teixeira, J.P. de Mesquita, R.R. Ribeiro, C.L. Donnici, R.M. Lago, Use of modified activated carbon for the oxidation of aqueous sulfide, *Carbon* 50 (2012) 1386–1393.
- [16] B.R.S. Lemos, I.F. Teixeira, B.F. Machado, M.R.A. Alves, J.P. de Mesquita, R.R. Ribeiro, R.R. Bacsas, P. Serp, R.M. Lago, Oxidized few layer graphene and graphite as metal-free catalysts for aqueous sulfide oxidation, *J. Mater. Chem. A* 1 (2013) 9491–9497.
- [17] Y. Wang, H. Zhao, M. Li, J. Fan, G. Zhao, Magnetic ordered mesoporous copper ferrite as a heterogeneous Fenton catalyst for the degradation of imidacloprid, *Appl. Catal. B: Environ.* 147 (2014) 534–545.
- [18] C.G. Ramankutty, S. Sugunan, Surface properties and catalytic activity of ferrosinels of nickel, cobalt and copper, prepared by soft chemical methods, *Appl. Catal. A* 218 (2001) 39–51.
- [19] J.A. Toledo-Antonio, N. Nava, M. Martínez, X. Bokhimi, Correlation between the magnetism of non-stoichiometric zinc ferrites and their catalytic activity for oxidative dehydrogenation of 1-butene, *Appl. Catal. A* 234 (2002) 137–144.
- [20] J.B. Silva, C.F. Diniz, R.M. Lago, N.D.S. Mohallem, Catalytic properties of nanocomposites based on cobalt ferrites dispersed in sol–gel silica, *J. Non-Cryst. Solids* 348 (2004) 201–204.
- [21] F.S.H. Abu-Samaha, M.I.M. Ismail, AC conductivity of nanoparticles $\text{Co}_x\text{Fe}_{1-x}\text{Fe}_2\text{O}_4$ ($x=0, 0.25$ and 1) ferrites, *Mater. Sci. Semicond. Process.* 19 (2014) 50–56.
- [22] G. Li, X. Ren, T. Dong, B. Yu, L. Guo, S. Yan, Preparation and characterization of the polyaniline nanocomposites with electricity/magnetic properties, *J. Macromol. Sci. Part B: Phys.* 48 (2009) 185–195.
- [23] J. Lee, S. Zhang, S. Sun, High-temperature solution-phase syntheses of metal–oxide nanocrystals, *Chem. Mater.* 25 (2013) 1293–1304.
- [24] A.S. Albuquerque, J.D. Ardisson, W.A.A. Macedo, J.L. Lopez, R. Paniago, A.I.C. Persiano, Structure and magnetic properties of nanostructured Ni-ferrite, *J. Magn. Magn. Mater.* 226–230 (2001) 1379–1381.
- [25] A.S. Albuquerque, M.V.C. Tolentino, J.D. Ardisson, F.C.C. Moura, R. de Mendonça, W.A.A. Macedo, Nanostructured ferrites: structural analysis and catalytic activity, *Ceram. Int.* 38 (2012) 2225–2231.
- [26] A.P.C. Teixeira, J.C. Tristão, M.H. Araujo, L.C.A. Oliveira, F.C.C. Moura, J.D. Ardisson, C.C. Amorim, R.M. Lago, Iron: a versatile element to produce materials for environmental applications, *J. Braz. Chem. Soc.* 23 (2012) 1579–1593.
- [27] C.A. Linkous, C. Huang, J.R. Fowler, UV photochemical oxidation of aqueous sodium sulfide to produce hydrogen and sulfur, *J. Photochem. Photobiol. A* 168 (2004) 153–160.
- [28] D.W. Tapley, G.R. Buettner, J.M. Shick, Free radicals and chemiluminescence as products of the spontaneous oxidation of sulfide in seawater, and their biological implications, *Biol. Bull.* 196 (1999) 52–56.
- [29] R.M. Silverstein, G.C. Bassler, T.C. Morrill, *Spectrometric Identification of Organic Compounds*, 3rd ed., Wiley, 1974.
- [30] K. Nakamoto, *Infrared and Raman Spectra of Inorganic and Coordination Compounds*, 3rd ed., John Wiley and Sons, 1978.
- [31] R.S. Hargrove, W. Kündig, Mössbauer measurements of magnetite below the Verwey transition, *Solid State Commun.* 8 (1970) 303–308.
- [32] L. Häggström, H. Annersten, T. Ericsson, R. Wäppling, W. Karner, S. Bjarman, Magnetic dipolar and electric quadrupolar effects on the Mössbauer spectra

- of magnetite above the Verwey transition, *Hyperfine Interact.* 5 (1977) 201–214.
- [33] M. Nippe, R.S. Khayzer, J.A. Panetier, D.Z. Zee, B.S. Olaiya, M. Head-Gordon, C.J. Chang, F.N. Castellano, J.R. Long, Catalytic proton reduction with transition metal complexes of the redox-active ligand bpy2PYMe, *Chem. Sci.* 4 (2013) 3934–3945.
- [34] I. Navarro-Solis, L. Villalba-Almendra, A. Alvarez-Gallegos, H₂ production by PEM electrolysis, assisted by textile effluent treatment and a solar photovoltaic cell, *Int. J. Hydrogen Energy* 35 (2010) 10833–10841.
- [35] Á. Nemes, G. Inzelt, Electrochemical and nanogravimetric studies of iron phthalocyanine microparticles immobilized on gold in acidic and neutral media, *J. Solid State Electrochem.* 18 (2014) 3327–3337.
- [36] J. Zhang, X. Wang, D. Qin, Z. Xue, X. Lu, Fabrication of iron-doped cobalt oxide nanocomposite films by electrodeposition and application as electrocatalyst for oxygen reduction reaction, *Appl. Surf. Sci.* 320 (2014) 73–82.
- [37] A.I. Vogel, *Textbook of Macro and Semimicro Qualitative Inorganic Analysis*, 5th ed., Longman Group Limited, London, 1979.